Single channel surface electromyogram deconvolution is a useful pre-processing for myoelectric control

Single channel surface electromyogram deconvolution is a useful pre-processing for myoelectric control

Maxime Bourges, Ganesh R. Naik, *Senior Member, IEEE,* and Luca Mesin

***Abstract*— *Objective:* Myoelectric control requires fast and stable identification of a movement from data recorded from a comfortable and straightforward system. *Methods:* We consider a new real-time pre-processing method applied to a single differential surface electromyogram (EMG): deconvolution, providing an estimation of the cumulative firings of motor units. A 2 channel-10 class finger movement problem has been investigated on 10 healthy subjects. We have compared raw EMG and deconvolution signals, as sources of information for two specific classifiers (based on either Support Vector Machines or k-Nearest Neighbours), with classical time-domain input features selected using Mutual Component Analysis. *Results:* Using the proposed pre-processing technique, classification performances statistically improve. For example, the true positive rates of the best-tested configurations were 80.9% and 86.3% when using the EMG and its deconvoluted signal, respectively. *Conclusion:* Even considering the limited dataset and range of classification approaches investigated, our preliminary results indicate the potential usefulness of the deconvolution pre-processing. *Significance:* Deconvolution of EMG is a fast pre-processing that could be easily embedded in different myoelectric control applications.**

***Index Terms*—Classification, Motor unit firing rate, Myoelectric control, Prostheses, Surface EMG**

I. Introduction

ELECTROMYOGRAM (EMG) has been widely used for prosthetic control since the 50's [1]. If the first attempts were simple on/off prostheses [2], the latest years have seen more complex systems emerging, with multiple degrees of freedom being controlled [3]. Researchers have proposed many classification techniques to reach this goal [4]. However, most of them follow the same scheme (Fig. 1), which can be split into the following steps.

1. Pre-processing raw EMG, e.g., filtering [5] and windowing time series [6].
2. Estimation of features, which can be extracted from different domains, e.g., time [7] [8], frequency [9], or time-frequency/time-scale [10].
3. Selection/reduction of the features set to avoid the curse of dimensionality. Unsupervised methods, such as Principal Component Analysis [11], or supervised techniques, like Uncorrelated Linear Discriminant Analysis (U-LDA) [12], have been applied.
4. Classification. Many different methods have been applied, for example, Support Vector Machines (SVM) [13], k Nearest Neighbours (kNN) [14], Neural Networks [15], Gaussian Mixtures Model (GMM) [16], Naïve Bayes (NB) [17].
5. Post-processing, e.g., majority voting [6] or Bayesian fusion [18].

This step flow can give great performances, with around 99% precision for some configurations [19]. The main axes of improvement are usually increasing the number of detection channels [19], finding new processing techniques instead of using more established ones [20], or optimizing one or several parameters [15]. However, increasing the number of surface electrodes could make the prosthesis expensive, cumbersome, and uncomfortable. Indeed, as the required performances of the prosthesis are constantly rising, many works are aimed at using few detection channels [21]. Moreover, optimizing the processing of the EMG could be prone to overfitting or the increase of the processing time, which should be kept low to allow for real-time control and be accepted by users. Indeed, the processing delay should be kept under 300 ms to ensure a good user's experience [6].

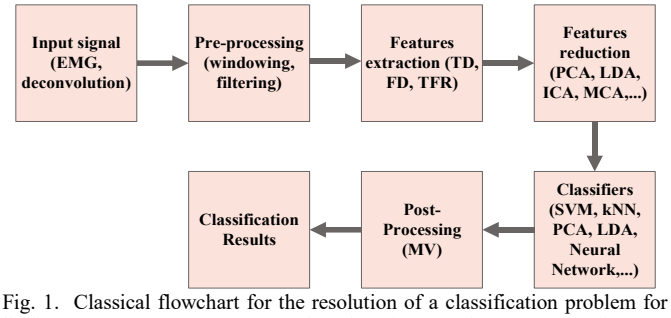

Fig. 1. Classical flowchart for the resolution of a classification problem for limb movements. Acronyms: TD - time domain, FD – frequency domain, TFR – time-frequency representations, PCA – principal components analysis, LDA – linear discriminant analysis, ICA – independent components analysis, MCA – mutual components analysis, SVM – support vector machine, kNN – k nearest neighbours, MV – majority voting.

Manuscript received …; revised ….

Asterisk indicates corresponding author.

M. Bourges and *L. Mesin are with the Mathematical Biology and Physiology group, Dip. di Elettronica e Telecomunicazioni, Politecnico di Torino, Corso Duca degli Abruzzi 24, Torino, 10129 Italy (e-mail: s262786@studenti.polito.it; luca.mesin@polito.it).

G. Naik is with the Flinders University, Bedford Park, South Australia, Australia (e-mail: Ganesh.Naik@flinders.edu.au).

Digital Object Identifier: …

An alternative is to get better information from the muscles. For example, intramuscular EMG provides selective information on motor unit (MU) recruitment of the target muscle and has provided good classification performances compared to surface EMG [22]. Indeed, surface EMG has a large detection volume and could present some problems, e.g., noise and crosstalk [23], that can degrade classification performances [5]. Classification based on other physical measures, such as force myography, are explored to overcome these problems, showing encouraging results [24]. Nevertheless, they usually require different hardware that is still less widespread than surface EMG amplifiers, which are instead available in most labs in the field of prosthetic control.

Thus, an innovative pre-processing of surface EMG could provide a step forward in the field of myoelectric control. This would keep the value of surface EMG technology (which is non-invasive and widespread), possibly providing a better input (e.g., in terms of selectivity of information, stability to noise, or crosstalk) to the classification machine.

Specifically, the timings of MU recruitment and discharges are related to muscle force [25] [26], velocity [27], and joint angle [28]. They have also been proposed for myoelectric control applications [29] [30]. Even if researchers have proposed solutions to get MUs discharge rates in real-time for prosthetic applications [31] [32], these approaches require a high-density recording system and intensive processing. As an alternative, a fast (real-time) and simple method has been proposed recently to estimate the cumulative activations of MUs from single differential (SD) recordings [33]. This paper is devoted to assessing if this pre-processing could help to increase the classification performances of a myoelectric prosthesis using a simple/low-density recording system.

II. METHODS

A. Data acquisition

The data collected in a previous study [18] have been used. The data were retrieved from [34]. In brief, the dataset includes EMGs from 10 subjects (2 were excluded in [18]), aged between 20 and 35 years old. No subject suffers from limb disability nor any neurological or muscular disorder. They have been seated on an armchair, allowing to support and fix their arm. The subjects were asked to perform ten classes of movement, i.e., individual and combined flexions of fingers: Thumb (T); Index (I); Middle (M); Ring (R); Little (L); Thumb and Index (TI); Thumb and Middle (TM); Thumb and Ring (TR); Thumb and Little (TL); Hand Closed (HC). These motions are shown in Fig. 2.

The subjects were instructed to contract their muscles from the rest position and hold the flexion for 5 seconds (the transition is included in the data, but not used here). Each movement was performed six times, with a resting time of 3-to-5 seconds in-between.

Four of these trials trained the classifier, whereas the other two formed the test set. Thus, the training set for each subject comprises 4 trials for 10 motor tasks (therefore 40 recordings of 5 s each), and the test set for each subject includes the remaining 20 recordings.

Surface EMG was recorded using two bipolar channels (Delsys DE 2.x series EMG sensors) and processed by the Bagnoli Desktop EMG Systems from Delsys Inc. A reference electrode has been attached to each subject's wrist and the two channels were placed near the elbow (Fig. 3; some more details and a picture is shown in [18]). The EMG was then amplified by a Delsys-Bagnoli-8 amplifier (total gain equal to 1000), sampled at 4000 Hz by a 12-bit analog-to-digital converter (National Instruments, BNC-2090) and acquired using Delsys EMGWorks Acquisition software. Fig. 4 shows examples of surface EMG data.

B. Deconvolution

The method proposed in [33] was used as pre-processing for each EMG channel before classification as an alternative to using the raw data. In short, surface EMG was approximately modelled as the convolution of a kernel and a cumulative sum of MU discharges (actually weighted by the amplitudes of motor unit action potentials - MUAPs):

$$s(t) = k(t) * x(t) \quad (1)$$

where $s(t)$ is the EMG signal, $k(t)$ is the kernel and $x(t)$ represents the cumulative firings to compute. Estimating the MU firings requires first selecting the kernel and then solving a deconvolution problem. As SD EMGs were considered, the first derivative of a Gaussian function was used as a kernel since it resembles the shape of MUAPs recorded in SD configuration. The variance of the Gaussian function was chosen so as the power spectral density (PSD) of the kernel best approximates that of the EMG. Indeed, the medium-high frequency spectrum of surface EMG reflects the average shapes of MUAPs [35].

The firing pattern convoluted with the kernel to fit the considered EMG was then estimated by deconvolution. This is an inverse problem whose solution is very unstable. Different methods have been proposed to get robust solutions to inverse problems, among which the Tikhonov approach was selected [36]. It consists in imposing (1) in a weak sense, i.e., reducing the mean squared error in fitting the model (right-hand side) to the data (left-hand side); moreover, the solution $x(t)$ is also constrained to have limited energy. The two requirements (of fitting data and restricting the energy of the solution) are linearly combined, writing an optimization problem, which requires reducing the following functional:

$$F(x) = \|s(t) - k(t) * x(t)\|_2^2 + \alpha\|x(t)\|_2^2 \quad (2)$$

Notice that the considered EMG is sampled so that the problem is discrete. Specifically, the convolution operation was written as the multiplication with a matrix A, collecting on its columns the kernel (discretized according to the sampling frequency) delayed by multiples of the sampling time. The penalty term α was set to 1% of the maximum eigenvalue of A^TA, thus limiting adequately the condition number of the matrix to be inverted to solve the deconvolution problem.

The energy functional is convenient, as it allows to get an analytical expression for the optimal solution. However, it is too affected by outliers and tolerant to small errors. L_1 optimization was introduced as a more robust alternative: it is less sensitive to significant errors and pushes small values to zero, providing sparse solutions [37], which better resemble MU firing patterns. However, there is no analytical solution for a least-L_1 problem. The Iterative Reweighted Least Squares (IRLS) method was applied to get an approximate solution [37]: the L_1 problem was

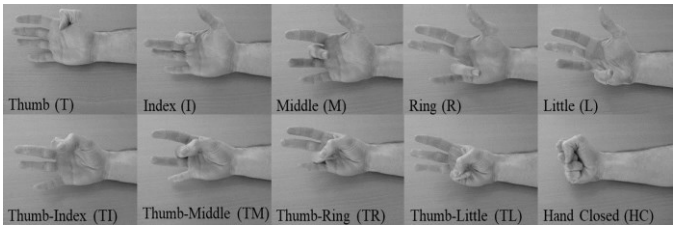

Fig. 2. Motions considered in this paper.

iteratively approximated by a weighted least squares problem at each step, for which an analytical solution exists. The weights were defined as the reciprocal of the L_1 error on each sample for the previous step. Thus, ideally, at convergence, the weighted squares problem becomes an L_1 problem (as the squared error is divided by the modulus of the error). As a compromise between accuracy and time cost, 10 iterations of this method were considered.

As an additional computation, before each iteration of the IRLS algorithm, the solution was set to zero when negative, since the firing pattern to be estimated must be non-negative.

Notice that the computational cost is quadratic with respect to the number of samples of the processed data, as matrix A has a dimension depending on its duration. Thus, it is convenient to split the time series to be processed in short sub-epochs. Specifically, our EMGs were split into sub-epochs of 20 ms; 5 ms of overlap was considered to avoid edge effects (see [33] for details).

Fig. 5 provides examples of deconvolution signals obtained by processing the EMGs shown in Fig. 4. Notice the low-frequency portion, which, according to the results shown in [33], should reflect the mean firing rate of MUs (weighted by MUAP amplitude). Some more examples are included in the Appendix.

C. Classification

The classical steps of EMG classification [4] are reminded in "Introduction" and Fig. 1. These steps were applied either to the raw EMG or to the signals obtained after deconvolution to understand if there is any advantage in using such a pre-processing. The details of the classification are described below.

1) Signal preparation

The following signals have been considered.

1. The raw EMG, notch filtered at 50 Hz and band-pass filtered between 20 Hz and 400 Hz. The attenuation is at least 30 dB in the stopband.

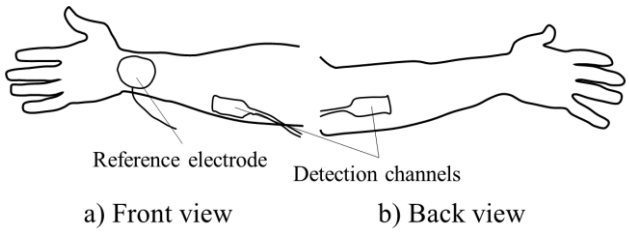

Fig. 3. Electrodes positions on the arm. The two acquisition channels are near the elbow, while the reference electrode is placed on the wrist.

2. The signal obtained by deconvolution of the EMG filtered by a notch at 50 Hz and band-pass filtered between 1 and 400 Hz (referred to as "deconvolution signal" in the following).

The EMG has traditionally been filtered these ways to cut the powerline interference (notch filter) and the noise [5]. Notice that, since we deconvoluted a previously filtered EMG, some noise is already excluded from the deconvolution we will use for the classification. No further filtering was added to the deconvolution since it would exclude important components (such as the low-frequency peak, which reflects the average firing rate [33]).

2) Signal processing

The signals were divided into several time windows of 250 ms, shifted by 50 ms. Using sliding instead of disjoint windows leads to better performances but requires more computation time. The minimum window increment for windows of this size is 16 ms [6], so we chose an increment of 50 ms to find a compromise between computation time and performance. We have extracted, for each window, some classical time-domain (TD) features from each channel [7] [8] [11] [38]: Mean Absolute Value (MAV), Root Mean Square (RMS), Zero Crossing (ZC), Slope Sign Change (SSC), Waveform Length (WL) and Integrated Absolute Value (IAV). The features set was then reduced using the Mutual Component Analysis (MCA) [3], which finds a compromise between the full information of the selected features and the minimum redundancy of the chosen set by optimizing the entropy of the features. It has been shown to offer good performance compared to other techniques [3]. Different reduced sets have been considered, containing respectively either 4, 6, or 8 features.

We have then applied two different classifiers among the most used in the literature: Support Vector Machine (SVM) [13] and k Nearest Neighbours (kNN) [14]. For the SVM, a

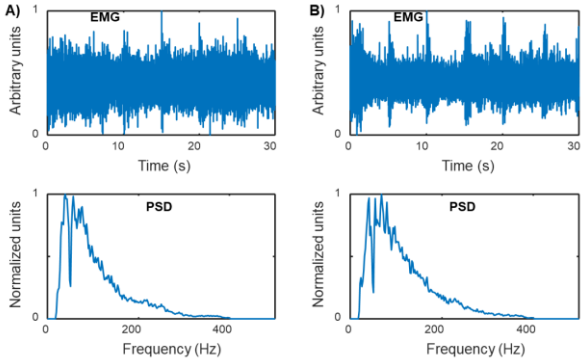

Fig. 4. Filtered EMG (top) and corresponding Power Spectral Density (PSD, bottom) recorded from subject 1 for the movement "Hand Closed". Six trials of five seconds each have been concatenated. The left column is the first channel (medial forearm), and the right column is the second (lateral forearm). A bandpass filter between 20 and 400 Hz and a notch at 50 Hz have been applied. The PSD is computed using the Welch method with Hamming windows of 0.5 s and an overlapping of 50%.

linear kernel was considered (similar results were obtained using a Gaussian kernel). Being a binary classifier, a "one-versus-one" strategy has been used to extend the algorithm to our multiclass problem. For K classes, K(K-1)/2 binary classifiers have been created, i.e., 45 in our study (K = 10

motions), and the assigned class is the one with the maximum number of "wins" from all classifiers. Concerning the kNN, the parameter k was empirically set to 5 after tuning on a few preliminary tests. A few additional tests are shown in the Appendix, considering LDA and NB classifiers.

Finally, a classical majority voter (MV) is applied as post-processing. The majority voter takes the output of the classifier as an input, which is the assigned class for each time window. The MV aims to smoothen the decisions of the classifier by averaging it over a certain number of windows. For example, for the n^{th} window with 5 decisions, the MV takes the five decisions between the $(n-2)^{th}$ and the $(n+2)^{th}$, and the output class for the n^{th} window is the one that appears the most in this span. By doing so, the MV eliminates spurious decisions. The controller delay must be kept under 300 ms for a real-time application [6]: here, we set the number of windows in the MV to 11, which is compatible with the maximum number of decisions (i.e., 13). Note that the maximum delay (which is related to the number of decisions) is not optimal for the average patient, which is in the 100-125 ms range [39]. However, we found after a preliminary check that sticking to this optimal delay (i.e., using only 5 decisions in the MV) would substantially increase the error rate with the selected classification scheme (some results indicating the effect of the number of windows included in the majority voting are shown in the Appendix).

To allow further analysis of the results, we computed some statistical measures of the performances of the classifiers depending on the number of features and the signal used. These

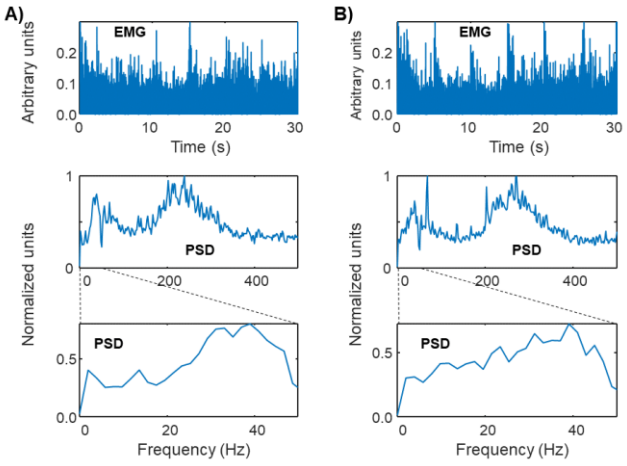

Fig. 5. Deconvolution signal (top) and its PSD (middle - all spectrum; bottom - low-frequency) obtained processing the signals shown in Fig. 4. The DC value was removed before estimating the PSD, which was computed using Welch method with Hamming windows of 0.5 s and overlapping of 50%.

measures are specificity, sensitivity, precision, accuracy, and F-score. Since they are defined for a binary classifier, we transformed the multiclass confusion matrix into one with only four outputs: True Positive (TP), False Positive (FP), True Negative (TN), and False Negative (FN). To do so, each class was successively considered as '1' and the other classes as '0' (one-vs-all approach). Thus, the TP scores indicate when the considered class is correctly classified; the FP scores are when another motion is classified as the considered class, and so on for the last two cases.

Moreover, we used two statistical tests to explore if the changes in performances when using the deconvolution signal instead of the EMG are statistically significant or due to chance. The first is the Wilcoxon sign rank test applied on the error rates for each subject, the second is the McNemar test [40] carried from the results for each time window (the output is either '1' for a well-classified motion or '0' for a misclassification). The tests were carried out with either the deconvolution signals or the EMGs, for both considered classifiers (i.e., SVM and kNN) and for 4, 6, and 8 features extracted by MCA.

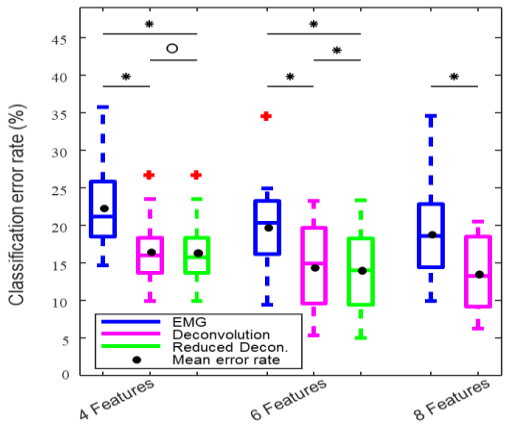

Fig. 6. Boxplots and mean classification error rate for TD features, SVM and MV with 11 decisions, depending on the number of features (selected by MCA) and the signal used (EMG, deconvolution or deconvolution with reduced feature set, i.e., including only Slope Sign Change, Waveform Length and Root Mean Square of the two channels). The bars above indicate a statistically significant difference between the classification outputs obtained from two different signals. The p-values were computed with McNemar test [40]. A circle and an asterisk indicate a p-value < 0.05 and < 0.01, respectively.

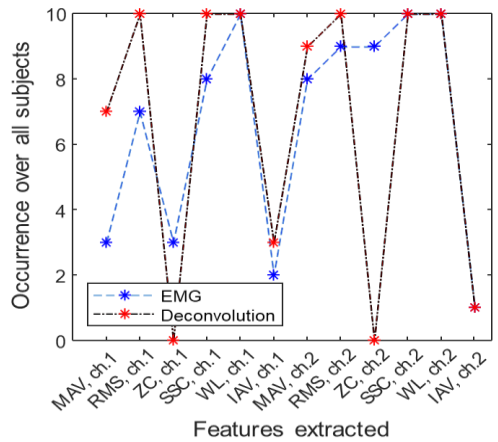

Fig. 7. Number of occurrences of every feature over 10 sets of features (one for each subject). These sets have been constructed by extracting the TD features introduced in the "Methods" section and by extracting 8 features by MCA for each subject.

III. Results

The error rate in classification with the SVM approach is displayed in Fig. 6 as a function of the number of features used (after MCA selection). Since the results for kNN follow the same trend as those obtained when using the SVM, but with lower average performances, they are not shown in Fig. 6 for the sake of simplicity (they are provided in the Appendix). The statistical measures of the performances are displayed in the Appendix (Table IV).

Notice that our results are not comparable to those obtained in [18], since different features are used here, and two patients had been excluded from the previous study, whereas we used them all.

We observe that, for every tested configuration, using the deconvolution leads to better average results than using the raw EMG filtered. Specifically, the mean error rate was reduced by 4-6% (for example, using 8 features and the SVM, the mean error rate is 19.06% with the features extracted from the EMG, whereas it is 13.74% when using data pre-processed by deconvolution).

The classification was run on Matlab 2019b, using some codes and toolboxes available on the internet [3] [38] [41] [42].

As expected, most of the classification errors come from the misinterpretation of motions involving the same fingers. For example, most of the errors when the subject makes R are misclassified as TR. Using the deconvolution, these misclassifications were reduced (as the mean error diminishes). However, the same trend is observable (see the confusion matrixes in the Appendix, considering the EMG with 8 features in Table V and the deconvolution with 8 features in Table VI). Thus, the classification based on the deconvolution signal does not entirely solve the confusion between "similar motions", even if it mitigates the problem in the average.

The boxplots in Fig. 6 and the standard deviation of the error rates (Table I) suggest that using the deconvolution signal also provides more robust classification outputs than raw EMG. In fact, the standard deviation is smaller when using the deconvolution: this means that the error rate is less keen to deviate from the mean. Indeed, when using the EMG to classify the motion task of the subjects, some aberrant results can occur (subject 3 is by far the most relevant example, with an error rate higher than 35% for all configurations).

TABLE I
STANDARD DEVIATION OF THE ERROR RATE AMONG ALL PARTICIPANTS DEPENDING ON THE SIGNAL USED FOR CLASSIFICATION

	Number of features	EMG	Deconvolution
SVM	4	5.91	5.38
	6	7.17	5.81
	8	7.36	4.93
kNN	4	7.23	4.92
	6	8.83	5.20
	8	8.22	5.46

TABLE II
RESULTS OF MCNEMAR TEST FOR STATISTICAL SIGNIFICANT IMPROVEMENT IN CLASSIFICATION RESULTS FROM DIFFERENT SIGNALS

Classifier	Number of features	EMG vs. Deconvolution	EMG vs. Reduced Decon.	Deconvolution vs. Reduced Decon.
SVM	4	$p < 0.001$	$p < 0.001$	$p = 0.0405$
	6	$p < 0.001$	$p < 0.001$	$p = 0.00216$
	8	$p < 0.001$	/	/
kNN	4	$p < 0.001$	$p < 0.001$	$p < 0.001$
	6	$p < 0.001$	$p < 0.001$	$p < 0.001$
	8	$p < 0.001$	/	/

Test carried on results for each time window (either '1' when correctly classified or '0' when misclassified) when using either EMG or deconvolution signal (with either complete or reduced feature set). Different classifiers, numbers of features selected by MCA and TD sets (either complete or reduced) are considered. Significant improvements of performance when using the deconvolution signal instead of the original EMG or the reduced deconvolution instead of the deconvolution (p-value lower than 0.05) are indicated in grey.

TABLE III
RESULTS OF WILCOXON SIGN RANK TEST FOR STATISTICAL SIGNIFICANT IMPROVEMENT IN CLASSIFICATION RESULTS FROM DIFFERENT SIGNALS

Classifier	Number of features	EMG vs. Deconvolution	EMG vs. Reduced Decon.	Deconvolution vs. Reduced Decon.
SVM	4	$p = 0.0371$	$p = 0.0195$	$p = 0.500$
	6	$p = 0.0371$	$p = 0.0273$	$p = 0.133$
	8	$p = 0.0098$	/	/
kNN	4	$p = 0.106$	$p = 0.0371$	$p = 0.300$
	6	$p = 0.0840$	$p = 0.0273$	$p = 0.412$
	8	$p = 0.0645$	/	/

Test carried on error rates when using either EMG or deconvolution signal (with either complete or reduced feature set). Same classifiers, feature selection methods and notations as in Table II.

We can further improve the classification algorithm by changing the feature set. When we look at the features selected mainly by the MCA algorithm (i.e., the most informative/lowest redundant) when classifying starting from the deconvolution signals (Fig. 7), we realize that the same ones are mostly used across all subjects. These features are the Slope Sign Change, the Waveform Length, and the Root Mean Square. On the contrary, the Zero Crossing features (estimated after removing the mean value), the Integrate Average Value, and the Mean Average Value are rarely used. A reduced set of features was then considered, including only these three features for the deconvolution signals (coming from the two channels), halving the number of features and decreasing the required computations. Such a distinction in the occurrences of the features was unclear when using the EMG, so this reduced feature set was considered only for the deconvolution signal. This new case is denoted as "reduced deconvolution".

The results are shown in Fig. 6: the performances are slightly better using only these 6 features (3 per channel) instead of the classical 12 (6 per channel). This solution seems to offer a good compromise between reduced computation and classification performances. Moreover, this choice could help reducing the risk of overfitting.

The p-values obtained from the two statistical tests are shown in Table II and Table III, respectively. When considering each time window (McNemar test, in Table II), the differences in the results obtained from different signals are statistically significant at a 95% confidence level. Most of the comparisons are even significant if we consider a 99% level of confidence.

Concerning the Wilcoxon test carried on the error rates (Table III), the size of the samples is relatively small, and outcomes are not that clear. For the SVM, the advantages of the deconvolution and the reduced deconvolution over the EMG can be statistically asserted at a 95% confidence level. Nevertheless, in the kNN case, the p-values obtained are too high to conclude statistical improvement in the performances when using the deconvolution instead of the EMG (even if median performances were better when pre-processing data by deconvolution). The comparison of the EMG and the reduced deconvolution, on the other hand, produces p-values below the chosen significance level of $\alpha = 0.05$. The p-values obtained

by comparing the deconvolution and the reduced deconvolution are above the chosen threshold in both SVM and kNN cases.

IV. Discussion

Improving myoelectric control is crucial in prosthesis design. To that extent, reducing the classification error rate is the priority in most researches [6] [16] [18] [19]. The prosthesis users identify as primary needs having an extensive range of degrees of freedom and performing everyday life tasks [43]. This requires precise control. Moreover, the myoelectric control should be fast to reduce the latency that would prevent a comfortable use of the prosthesis [6].

TABLE IV
STATISTICAL MEASURES OF THE PERFORMANCES OF THE SVM FOR EACH SIGNAL, DEPENDING ON THE NUMBER OF FEATURES.

N.feat	Signal	Sensitivity	Specificity	Precision	Accuracy	F-score
4	EMG	0.775	0.975	0.775	0.955	0.775
	Deconv	0.833	0.981	0.833	0.967	0.833
	Red Decon.	0.834	0.982	0.834	0.967	0.834
6	EMG	0.801	0.978	0.801	0.960	0.801
	Deconv	0.854	0.984	0.854	0.971	0.854
	Red Decon.	0.857	0.984	0.857	0.972	0.857
8	EMG	0.809	0.979	0.810	0.962	0.809
	Deconv	0.863	0.985	0.863	0.973	0.863

Performances of SVM calculated by micro-averaging: the confusion matrix of the multiclass problem was transformed in a simple confusion matrix of a binary classifier by successively considering each class as '1' and all the others as '0' (one-vs-all).

This paper introduces an innovative method for prosthesis control based on a pre-processing of surface EMG: the single-channel deconvolution. This preliminary processing, which can be performed in real-time [33], leads to better classification results than raw data.

The deconvolution provides an estimation of the MU cumulative firing rate. Thus, it allows to emphasize the information provided by MU firing patterns. An extension of this method has been recently introduced [44]: more convolution kernels are used, accommodating shape variations of MUAPs. This is very important in case of phase changes in the MUAPs (mainly found if there are multiple innervation zones or in case of fibre pinnation). However, this improved algorithm has a larger computational time, precluding the real-time application needed for our application. Deconvoluting the EMG gives access to more informative signals related to MU activities. Specifically, low-frequency contributions provide information on the average MU firing rate [33]. In contrast, high-frequency components allow the signal to be spiky, better reflecting MU firings, which could discriminate better the different motor tasks. Moreover, ideally compensating for MUAP shapes, the method could be stable to myoelectric manifestations of peripheral fatigue (reflected by slowing the velocity of propagation of the action potentials along muscle fibres [45]). A possible alternative to deconvolution is the decomposition by spike sorting approaches [46] [47]. A real time method has been proposed [46], but it does not resolve overlaps of different waveforms (which are so important in surface EMG); on the opposite side, methods resolving overlaps are available, but they are very intensive [47]. Other methods to get MU firings from surface EMG and to use them in a prosthesis control frame had been used in the literature [29] [30]. Nonetheless, these methods are based on high-density detection arrays and blind source separation techniques, requiring intensive processing. Instead, the deconvolution estimates the cumulative firing pattern from a single detection channel and in real-time. Thus, the controlling method introduced in this paper appears to be simpler, faster and cheaper than the pre-existing ones.

Another advantage of this new technique compared to the raw EMG is the robustness toward the different subjects, as shown by a lower standard deviation on classification error rates. The high variation of the classification performances over the patients when using the raw EMG can be due to many factors, e.g., a displacement of an electrode, an unusual noise, or differences in the patients' anatomy, reflecting on different MUAP shapes. On the contrary, we have obtained more stable results across subjects when using the deconvolution (which ideally compensates for different MUAP shapes across subjects, preserving only information on firings).

As shown in Tables II and III, statistically significant improvements of classification performance when including the proposed pre-processing are asserted in many cases. When using the reduced deconvolution instead of the EMG, the null hypothesis can be rejected with a 95% confidence level for both considered classifiers (SVM and kNN). That is also the case for the deconvolution compared to the EMG for the SVM. We can conclude that there are statistically significant improvements in these cases. On the other hand, when comparing the performances of kNN using either EMG or deconvolution signals, the p-values are too high to conclude at the chosen level of confidence. Nevertheless, lower median classification rates were still consistently obtained when using the deconvolution signal, independent of the included features. Note that no statistical improvement between the deconvolution and the reduced deconvolution can be asserted at the given confidence level. This is undoubtedly due to the closeness of the information extracted. Indeed, the set of reduced features appeared the most after the MCA was applied to the indexes extracted from the deconvoluted signal. Thus, most information sent to the classifier is the same for the deconvolution and the reduced deconvolution, and the differences in the results are not statistically different. Nevertheless, the reduction of the set has the advantages we explained earlier.

Even considering these promising results, our study has many limitations. For example, as we mentioned in the "Results" section, some confusion between classes was found when the same fingers were in motion (e.g., between TL and L, or TR and R: see Table V in Appendix). Despite the reduction of the confusion, it is not entirely solved when using the proposed pre-processing. We can speculate that the cumulative firing rate in those motions, e.g., to bend the ring finger alone or together with the thumb, will be similar, thus inducing some misclassifications. Further information could be needed to improve the discrimination capability of our classifier. Some methods have also been introduced to discriminate simultaneous motions [48]: possibly, applying such approaches to the deconvolution signal could improve the classification performances.

Moreover, we have focused on particular classification approaches, considering specific features, a selection method, and two classical classifiers (some tests considering other classifiers are shown in the Appendix). For example, only one domain of features (TD) has been considered. As we mentioned earlier, many other domains are used in the literature, and some studies showed excellent classification results [10] [19]. Moreover, different feature generation/selection approaches could be used, as well as different classifiers. Thus, there is room for improving the classification performances. However, here we are not concerned with the aim of getting the best possible performances with our data, but only with the assessment of the importance of using the EMG pre-processing by deconvolution. Even being aware that many different alternative classification approaches could be used, our tests clearly show the potential of our pre-processing, which allows us to get improved and more stable performances across subjects when considering classical features and classifiers often used in myoelectric control.

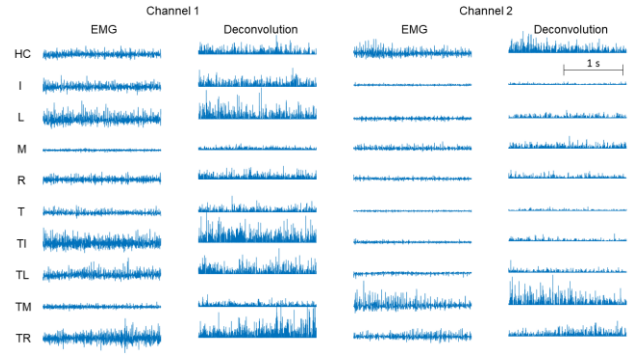

Fig. 8. Portion of data (EMG and corresponding deconvolution signal) for each executed movement (acronyms defined in Fig. 2).

We should also notice that the data we used here were recorded in laboratory conditions. Researchers have noted how different the results can be between these conditions and daily life [49]. The subjects' arms were on a support, in a given position that was the same for all trials. Thus, we cannot conclude the robustness toward an electrode misplacement or a different arm position. Moreover, the effect of fatigue was not investigated. Both central and peripheral myoelectric manifestations of fatigue have been documented [45]. As mentioned above, the deconvolution signal ideally reflects central control, compensating for MUAPs shapes (changing as a peripheral manifestation of fatigue); we can then speculate that it could be affected to a lesser extent with respect to the raw EMG (which is affected both by central and peripheral fatigue). These aspects should be explored in the future.

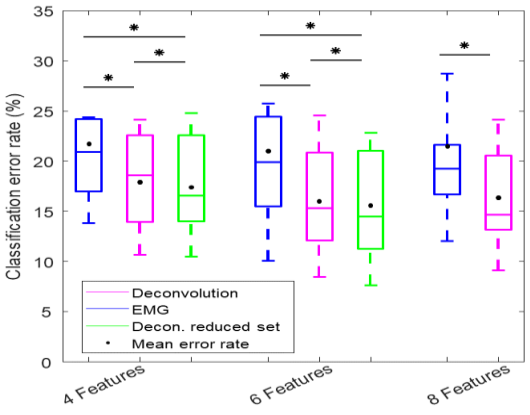

Fig 9. Error rates for the kNN classifier (same notation as for Fig. 6).

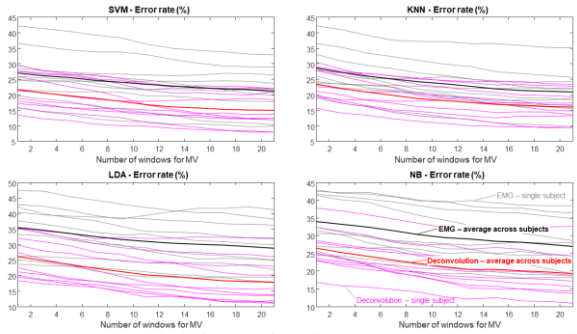

Fig. 10. Error rate of different classifiers (SVM, kNN, LDA and NB) considering 6 features (selected by MCA) and different numbers of windows for the majority voting. Filtered EMG and deconvolution are considered, both showing single subjects and the average error rate across them.

Also, note that some researchers, especially from the industry, claim that other improvements beyond the classification rate should be sought, such as providing sensory feedback [50] or adapting to EMG changes (due to fatigue, sweat,…) and being more robust toward non-ideal conditions [50] [51]. These are other vital points to be addressed in the future, in addition to the need of reducing the execution time [6].

Nevertheless, besides the limitations of our work, the proposed method is promising because it overcomes the EMG in the classification process without needing complex detection and keeping low the computational cost. It seems to be a path to follow in the future to improve prosthesis control. For example, the proposed pre-processing could be integrated into other advanced methods, such as those focused on force and pattern classification [52].

TABLE V
CONFUSION MATRIX OF THE MOVEMENT CLASSIFICATION BY SVM/DECONVOLUTION USING THE EMG WITH 8 FEATURES.

		Estimated movement									
		HC	I	L	M	R	T	TI	TL	TM	TR
Executed movement	HC	1859/1895	0/3	0/0	5/0	52/7	3/0	0/0	1/0	0/0	0/15
	I	8/12	1323/1575	16/30	40/4	49/54	215/93	259/134	10/18	0/0	0/0
	L	0/11	26/3	1395/1600	2/7	1/3	109/20	34/28	324/166	17/19	12/63
	M	72/17	3/0	13/15	1689/1745	8/2	0/32	11/0	0/52	89/6	35/51
	R	6/19	0/5	0/10	4/9	1733/1676	54/2	0/0	0/17	0/7	123/175
	T	36/22	214/166	78/49	4/20	8/1	1558/1554	1/42	0/20	9/11	12/35
	TI	0/0	129/39	60/47	206/41	9/0	96/72	1365/1677	24/35	19/9	12/0
	TL	0/0	12/8	246/129	64/127	9/0	0/25	8/11	1392/1573	145/6	44/41
	TM	11/8	4/0	45/54	16/22	2/20	0/19	0/0	54/43	1780/1729	8/25
	TR	5/41	0/0	26/1	0/32	376/232	3/10	34/0	28/66	2/0	1446/1538

All epochs from all subjects have been considered. The rows are the expected motions, and the columns are the output of the classification.

V. Conclusion

Using the single-channel deconvolution instead of the raw EMG improves the myoelectric control. The error rate in motion task identification is significantly reduced (around a 5% cut through all subjects). The method is promising, as it does not require any complex detection system, and the processing can be performed in real-time. The performances are also more homogenous among the investigated subjects. Using this signal also reduces inputs when considering the usual time-domain features, decreasing the computational cost. Additional tests are needed to check the feasibility of this approach in realistic conditions.

Appendix

Figure 8 shows the EMG and deconvolution of an epoch for each gesture. Detailed results are provided in Tables IV-VI, showing, respectively, different performance indexes of SVM classifier (Table IV) and the confusion matrices when using either the EMGs or the deconvolution signals (Table V). Moreover, Figure 9 shows the error rate distribution of kNN classifier. The effect of the number of windows included in the majority voting is investigated in Figure 10, considering LDA and NB as classification approaches, in addition to SVM and kNN.

References

[1] D. McKenzie, "The Russian Myoelectric Arm," The Journal of bone and joint surgery. *British volume*, vol. 47, pp. 418—420, 1965.

[2] P. Geethanjali, "Myoelectric control of prosthetic hands: state-of-the-art review," *Medical devices* (Auckland, N.Z.), vol. 9, pp. 247—255, 2016.

[3] R. Khushaba and S. Kodagoda, "Electromyogram (EMG) feature reduction using Mutual Components Analysis for multifunction prosthetic fingers control," *2012 12th International Conference on Control Automation Robotics & Vision (ICARCV)*, 2012, pp. 1534-1539.

[4] N. Parajuli, N. Sreenivasan, P. Bifulco, M. Cesarelli, S. Savino, V. Niola, D. Esposito, T. Hamilton, G. Naik, U. Gunawardana and G. Gargiulo, "Real-Time EMG Based Pattern Recognition Control for Hand Prostheses: A Review on Existing Methods, Challenges and Future Implementation," *Sensors* (Basel), vol. 19, p. 4596, 2019.

[5] R. Chowdhury, "Surface Electromyography Signal Processing and Classification Techniques," *Sensors*, vol. 13, pp. 12431-12466, 2013.

[6] K. Englehart and B. Hudgins, "A Robust, Real-Time Control Scheme for Multifunction Myoelectric Control," *IEEE Trans on Biomed Eng*, vol. 50, pp. 848-54, 2003.

[7] M. Zardoshti-Kermani, B. C. Wheeler, K. Badie and R. M. Hashemi, "EMG feature evaluation for movement control of upper extremity prostheses," *IEEE Trans on Rehab Eng*, vol. 3, pp. 324-333, 1995.

[8] B. Hudgins, P. Parker and R. Scott, "A new strategy for multifunction myoelectric control," *IEEE Trans on Biomed Eng*, vol. 40, pp. 82-94, 1993.

[9] K. A. Farry, I. D. Walker and R. G. Baraniuk, "Myoelectric teleoperation of a complex robotic hand," *IEEE Trans on Robotics and Automation*, vol. 12, pp. 775-788, 1996.

[10] K. Englehart, B. Hudgins, P. Parker and M. Stevenson, "Classification of the myoelectric signal using time-frequency based representations," *Medical engineering & physics*, vol. 21, pp. 431-8, 1999.

[11] C. Li, J. Ren, H. Huang, B. Wang, Y. Zhu and H. Hu, "PCA and deep learning based myoelectric grasping control of a prosthetic hand," *BioMedical Engineering OnLine*, vol. 17, 2018.

[12] J. Ye, R. Janardan, Q. Li and H. Park, "Feature extraction via generalized uncorrelated linear discriminant analysis," *21th International Conference on Machine learning* (ICML '04), New-York, NY, USA, 2004.

[13] N. Güler and S. Kocer, "Classification of EMG signals using PCA and FFT," *Journal of medical systems*, vol. 29, pp. 241-50, 2005.

[14] C. Cipriani, C. Antfolk, M. Controzzi, G. Lundborg, B. Rosén, M. Carrozza and F. Sebelius, "Online Myoelectric Control of a Dexterous Hand Prosthesis by Transradial Amputees," *IEEE Trans on Neural Systems and Rehab Eng*, vol. 19, pp. 260-70, 2011.

[15] M. R. Ahsan, M. Ibrahimy and O. Khalifa, "Optimization of Neural Network for Efficient EMG Signal Classification," *8th International Symposium on Mechatronics and its Applications*, 2012.

[16] Y. Huang, K. Englehart, B. Hudgins and A. Chan, "A Gaussian Mixture Model Based Classification Scheme for Myoelectric Control of Powered Upper Limb Prostheses," *IEEE Trans on Biomed Eng*, vol. 52, pp. 1801-11, 2005.

[17] Z. Lu, A. Stampas, G. Francisco and P. Zhou, "Offline and online myoelectric pattern recognition analysis and real-time control of a robotic hand after spinal cord injury," *J Neural Eng.*, vol. 16, no. 13, p. 036018, 2019.

[18] R. Khushaba, S. Kodagoda, M. Takruri and G. Dissanayake, "Toward Improved Control of Prosthetic Fingers Using Surface Electromyogram (EMG) Signals," *Expert Systems with Applications*, vol. 39, p. 10731–10738, 2012.

[19] K. Englehart, B. Hudgins and P. Parker, "A wavelet-based continuous classification scheme for multifunction myoelectric control," *IEEE Trans on Biomed Eng*, vol. 48, pp. 302-11, 2001.

[20] M. Khezri and M. Jahed, "Real-time intelligent pattern recognition algorithm for surface EMG signals," *Biomedical Engineering Online*, vol. 6, p. 45, 2007.

[21] M. Tavakoli, C. Benussi and J. Lourenco, "Single Channel Surface EMG Control of Advanced Prosthetic Hands: A Simple, Low Cost and Efficient Approach," *Expert Systems with Applications*, vol. 79, 2017.

[22] T. Farrell and R. Weir, "Pilot comparison of surface vs. implanted EMG for multifunctional prosthesis control," *Proceedings of the 2005 IEEE 9th International Conference on Rehabilitation Robotics*, Chicago, IL, USA, 2005.

[23] L. Mesin, "Crosstalk in surface electromyogram: literature review and some insights," *Phys Eng Sci Med*, vol. 43, no. 12, pp. 481–492, 2020.

[24] A. Belyea, K. Englehart and E. Scheme, "FMG vs EMG: A Comparison of Usability for Real-time Pattern Recognition Based Control," *IEEE Trans on Biomed Eng*, vol. 66, no. 11, pp. 3098-3104, 2019.

[25] R. Enoka and J. Duchateau, "Rate Coding and the Control of Muscle Force," *Cold Spring Harbor Perspectives in Medicine*, vol. 7, 2017.

[26] X. Zhang, G. Zhu, M. Chen, X. Chen, X. Chen and P. Zhou, "Muscle Force Estimation Based on Neural Drive Information From Individual Motor Units," *IEEE Transactions on Neural Systems and Rehab Eng*, vol. 28, no. 112, pp. 3148-3157, 2020.

[27] A. Vecchio, F. Negro, A. Holobar, A. Casolo, J. P. Folland, F. Felici and D. Farina, "You are as fast as your motor neurons: speed of recruitment and maximal discharge of motor neurons determine the maximal rate of force development in humans," *The Journal of Physiology*, vol. 597, no. 9, pp. 2445-2456, 2019.

[28] C. Dai and X. Hu, "Finger Joint Angle Estimation Based on Motoneuron Discharge Activities," *IEEE J Biomed Health Inform*., vol. 24, no. 13, pp. 760-767, 2020.

[29] T. Kapelner, F. Negro, O. C. Aszmann, Farina and D., "Decoding Motor Unit Activity From Forearm Muscles: Perspectives for Myoelectric Control," *IEEE Transactions on Neural Systems and Rehab Eng*, vol. 26, pp. 244-251, 2018.

[30] C. Chen, G. Chai, W. Guo, X. Sheng, D. Farina and X. Zhu, "Prediction of finger kinematics from discharge timings of motor units: implications for intuitive control of myoelectric prostheses," *Journal of Neural Engineering*, vol. 16, 2018.

[31] C. Chen, Y. Yu, X. Sheng, D. Farina and X. Zhu, "Simultaneous and proportional control of wrist and hand movements by decoding motor unit discharges in real time," *Journal of Neural Engineering*, vol. 18, 2021.

[32] I. Mendez, D. Barsakcioglu, I. Vujaklija, D. Wetmore and D. Farina, "Non-invasive real-time access to the output of the spinal cord via a wrist wearable interface," *bioRxiv*, 2021.

[33] L. Mesin, "Single channel surface electromyogram deconvolution to explore motor unit discharges," *Medical & Biological Engineering & Computing*, vol. 57, no. 9, pp. 2045-2054, 2019.

[34] R. Khushaba. Available: https://www.rami-khushaba.com. [Accès le 02 03 2020].

[35] C. De Luca, "Physiology and mathematics of myoelectric signals.," *IEEE Trans Biomed Eng*., vol. 26, no. 16, pp. 313-25., 1979.

[36] A. A. V. Tikhonov, Solution of ill-posed problems, New-York: Wiley, 1977.

[37] C. Burrus, "Iterative Reweighted Least Squares *," 2014.

[38] A. Chan and G. Green, "Myoelectric control development toolbox," *30th Conference of the Canadian Medical & Biological Engineering Society*, Toronto, Canada, 2007.

[39] T. Farrell and R. Weir, "The Optimal Controller Delay for Myoelectric Prostheses,", *IEEE Transactions on Neural Systems and Rehab Eng*, vol. 15, pp. 111 - 118, 04 2007.

[40] G. Cardillo, "McNemar test," 2021. Available: https://github.com/dnafinder/mcnemar.

[41] R. N. Khushaba, A. Al-Jumaily and A. Al-Ani, "Novel Feature Extraction Method based on Fuzzy Entropy and Wavelet Packet Transform for Myoelectric Control," *7th International Symposium on Communications and Information Technologies* ISCIT2007, Sydney, Australia, 2007.

[42] I. Nabney, "MATLAB Central File Exchange-Netlab," Available: https://www.mathworks.com/matlabcentral/fileexchange/2654-netlab.

[43] F. Cordella, A. Ciancio, R. Sacchetti, A. Davalli, A. Cutti, E. Guglielmelli and L. Zollo, "Literature Review on Needs of Upper Limb Prosthesis Users," *Frontiers in Neuroscience*, vol. 10, 2016.

[44] L. Mesin, "Motor Unit Discharges from Multi-Kernel Deconvolution of Single Channel Surface Electromyogram," *Electronics*, vol. 10, p. 2022, 2021.

[45] L. Mesin, D. Dardanello, A. Rainoldi and G. Boccia, "Motor unit firing rates and synchronisation affect the fractal dimension of simulated surface electromyogram during isometric/isotonic contraction of vastus lateralis muscle," *Medical Engineering & Physics*, vol. 38, pp. 1530-1533, 2016.

[46] S. Karimimehr, H. Marateb, S. Muceli, M. Mansourian, M. Mañanas and D. Farina, "A Real-Time Method for Decoding the Neural Drive to Muscles Using Single-Channel Intra-Muscular EMG Recordings.," *Int J Neural Syst.*, vol. 27, no. 16, p. 1750025, 2017.

[47] G. Chiarion and L. Mesin, "Resolution of Spike Overlapping by Biogeography-Based Optimization," *Electronics*, vol. 10, no. 112, p. 1469, 2021.

[48] A. J. Young, L. H. Smith, E. J. Rousse and L. J. Hargrove, "Classification of Simultaneous Movements Using Surface EMG Pattern Recognition," *IEEE Trans on Biomed Eng*, vol. 60, pp. 1250-1258, 2013.

[49] E. Campbell, A. Phinyomark and E. Scheme, "Current Trends and Confounding Factors in Myoelectric Control: Limb Position and Contraction Intensity," *Sensors* (Basel), 2020.

[50] N. Jiang, S. Dosen, K. Muller and D. Farina, "Myoelectric Control of Artificial Limbs—Is There a Need to Change Focus?," *IEEE Signal Processing Magazine*, vol. 29, pp. 152-150, 2012.

[51] O. Samuel, M. Asogbon, Y. Geng, A. Al-Timemy, S. Pirbhulal, N. Ji, S. Chen, P. Fang and G. Li, "Intelligent EMG Pattern Recognition Control Method for Upper-Limb Multifunctional Prostheses: Advances, Current Challenges, and Future Prospects," *IEEE Access*, vol. 7, pp. 10150-10165, 2019.

[52] C. Castellini and P. van der Smagt, "Surface EMG in advanced hand prosthetics," *Biological cybernetics*, vol. 100, pp. 35-47, 2008.